Reviews

Syntheses and Structures of Organically Templated Iron Phosphates

Kwang-Hwa Lii,*,† Yuh-Feng Huang,† Vítezslav Zima,† Chih-Yuan Huang,† Hsiu-Mei Lin,† Yau-Chen Jiang,‡ Fen-Ling Liao,‡ and Sue-Lein Wang‡

Institute of Chemistry, Academia Sinica, Taipei, Taiwan, R.O.C, and Department of Chemistry, National Tsing Hua University, Hsinchu, Taiwan, R.O.C

Received March 9, 1998. Revised Manuscript Received May 5, 1998

Iron phosphates are of interest because of rich crystal chemistry and practical applications. New crystalline iron phosphates have been prepared in aqueous or predominantly nonaqueous solvents under mild hydrothermal conditions using organic amines as structure-directing agents. The effects of pH, solvent, and temperature on the reaction products are discussed. FePOs have been prepared with 1-D chain, 2-D layered, and 3-D open framework structures. An FePO containing a chiral amine is also synthesized. This review will summarize some of the results of the work in the area of organically templated iron phosphates.

Contents

Introduction

Naturally occurring iron phosphate minerals have a rich crystal chemistry, and according to Moore, they are among the most perplexing substances in the mineral kingdom.[1] A large number of structurally diverse examples of both open and dense octahedral−tetrahedral frameworks have been reported. Perhaps the most famous example among these phosphate minerals is the structure of cacoxenite, which contains enormous channels of 14.2 Å, which are filled with unlocated water molecules.[2] A large number of synthetic iron phosphates have also been reported. They include binary compounds in the Fe−P−O system and ternary compounds with metal cation templates in the iron phosphate framework voids.[3,4] Synthetic iron phosphates are of interest not only for the diversity of their structural chemistry, but also for many applications in catalysis. For example, iron phosphates are known to selectively catalyze the oxidative dehydrogenation of isobutyric acid to methacrylic acid, which is a raw material for various polymers.[5,6] The industrial iron phosphate catalyst is a mixture of several phases which are prepared under conditions where only the products with compact crystal structures are obtained. Consequently, iron phosphates with micropores large enough to sorb organic molecules are of great interest from the viewpoint of catalysis.

The preparation of iron phosphates calls upon several methods: hydrothermal growth, fluoride flux, chemical vapor transport, or simply prolonged heating.[3] Among these synthetic methods, the hydrothermal techniques appear to be most versatile. Hydrothermal synthesis involves the use of aqueous solvents or mineralizers under high temperature and high pressure to dissolve and recrystallize materials that are relatively insoluble under ordinary conditions. The synthesis exploits the principle of "self-assembly" of the metastable solid phase from soluble precursors. For reaction temperatures above 300 °C, steel reaction vessels are used. A noble metal liner or plating is used to prevent corrosion. A large number of iron phosphates with metal cation templates have been prepared under high-temperature, high-pressure hydrothermal conditions.[4] However, the high temperature precludes the use of organic templates, and therefore one must use an inorganic cation. A cationic organic template, which is larger than inorganic cations, can leave a micropore large enough to sorb molecules if it can be removed from the framework. The presence of large cavities in the open framework structures may provide a large internal surface area and thus a large number of catalytic sites. Consequently, a mild hydrothermal approach, as in the case of the synthesis of zeolites, becomes necessary. For reactions in water or organic solvents at 100−200 °C under autogenous pressure, autoclaves with Teflon liners are particularly advantageous because Teflon resists both acidic and alkaline media and the vessel is easily assembled and taken apart. More importantly in the present case would be the possibility of incorporating organic cations of appropriate size or geometry to fill the voids in the structures. Although a very large

† Academia Sinica.
‡ National Tsing Hua University

10.1021/cm980152h CCC: $15.00
Published on Web 09/18/1998

number of organically templated transition metal phosphates have been reported for molybdenum and vanadium,[7,8] few examples of iron phosphate frameworks were known. With the examples of the open-framework iron phosphate mineral structures as encouragement, we began to investigate the hydrothermal syntheses of iron phosphates to try to incorporate larger removable organic cations. We review here recent developments in the system, first the synthesis and then the structures.

Synthesis

The syntheses were performed by heating iron chlorides or nitrates, amines, and phosphoric acid in appropriate proportions in water or a mixture of water and organic solvents in Teflon-lined autoclaves at temperatures ranging from 110 to 180 °C for several days followed by slow cooling. The syntheses have so many parameters (time, temperature, relative concentrations of reactants, pH, starting materials, etc.) that it is difficult to navigate through the enormous parameter space. Subtle changes in the reaction conditions can greatly affect the course of the reactions. Several variables have to be kept constant in this exploratory synthesis. Thus $FeCl_3 \cdot 6H_2O$, $FeCl_2 \cdot 4H_2O$, and H_3PO_4 (85% aqueous) were used as the sources of iron and phosphorus. $Fe(NO_3)_3 \cdot 6H_2O$, which appears to be less hygroscopic than the chloride, can also be used. The properties of solvents are often vital to the success or failure of the attempted syntheses. Both aqueous and nonaqueous solvents, such as 1-butanol and ethylene glycol, have been used in the synthesis. Alcohols and diols are less effective than water in hydrogen-bonding ability, and so there is a greater interaction between the framework particles and the templates. Both butanol and ethylene glycol have higher viscosity than water, and this may reduce convection currents and help produce large single crystals rather than polycrystalline product by sedimentation.[9]

The choice of pH is also critical to the outcome of the synthesis of iron phosphates. It is instructive to examine the effect that changing pH will have on the aqueous chemistry of iron. The hexaaquo ion $[Fe(H_2O)_6]^{2+}$ is readily formed upon simple dissolution of Fe^{II} salts in water.[10] Hydrolysis of $[Fe(H_2O)_6]^{2+}$ is not extensive and only occurs at alkaline pH. Only mononuclear hydrolysis product is formed and hydrous $Fe(OH)_2$ precipitates at around pH 10. In contrast, the smaller ionic size of Fe^{3+} leads to extensive hydrolysis of its aqueous solutions. Even in strongly acidic solutions (several molar in $[H^+]$), the pale purple ion $[Fe(H_2O)_6]^{3+}$ takes on yellow coloration arising from species taking part in the slow and complex set of equilibria that are involved in the hydrolytic polymerization process. The hydrolysis of $[Fe(H_2O)_6]^{3+}$ in acidic solution involves the main equilibrium:

$$[Fe(H_2O)_6]^{3+} = [Fe(OH)(H_2O)_5]^{2+} + H^+ \qquad K = 10^{-3.05}$$

A small amount of $[Fe(OH)_2(H_2O)_4]^+$ may be formed, but the second main species is the dimer:

$$2[Fe(OH)(H_2O)_5]^{2+} = [(H_2O)_5FeOFe(H_2O)_5]^{4+} + H_2O \qquad K = 10^{-2.91}$$

As the pH is raised above 2 or 3, further condensation occurs, colloidal gels begin to form, and eventually a reddish-brown precipitate of hydrous iron oxide is formed. It is evident therefore that Fe^{III} salts dissolved in water produce highly acidic solutions.

The mechanism of hydrothermal synthesis of microporous materials is poorly understood. However, it is reasonable to propose that microporous material nucleates within a gel particle and the organization of inorganic anions around the organic cation forms the basis of the nucleation centers from which the iron phosphate crystallites form. The synthesis of large pores may be through the use of large organic templates. Although it remains unknown how the structures are assembled at the molecular level, larger inorganic building units should also lead to large pores. One can imagine the construction of three-dimensional iron phosphate frameworks with large pores from gel precursors that already contain polynuclear iron−oxygen species. It is clear from earlier discussion that hexaaquo iron(III) complexes condense to high molecular weight species as the pH increases. Therefore, iron phosphate gel precursors with initial pH values in the region 5−10 have been used in our exploratory synthesis. In the following the synthesis, conditions for $[H_3N(CH_2)_3NH_3]_2[Fe_4(OH)_3(HPO_4)_2(PO_4)_3] \cdot xH_2O$ and $[H_3N(CH_2)_3NH_3][Fe_2O(PO_4)_2]$ are described to show the effects of pH, solvent, and reaction temperature.[11,12]

Excess organic amine and phosphoric acid were used as mineralizers, and the pH of the reaction mixture was largely determined by the amine/H_3PO_4 molar ratio. $FeCl_3 \cdot 6H_2O$ or $Fe(NO_3)_3 \cdot 6H_2O$ was used as the source of iron because they are soluble in water. In the synthesis of $[H_3N(CH_2)_3NH_3]_2[Fe_4(OH)_3(HPO_4)_2(PO_4)_3] \cdot xH_2O$, 7.5 mmol of 1,3-diaminopropane was slowly added with stirring to a solution of 1.5 mmol of $FeCl_3 \cdot 6H_2O$, 7.5 mmol of H_3PO_4, and 10 mL of water. The final reaction mixture was a light yellow homogeneous gel and had an initial pH value about 6. The gel was sealed in a Teflon-lined stainless steel autoclave, heated under autogenous pressure at 165 °C for 3 days, and cooled to room temperature at 10 °C/h. The final pH remained ca. 6. The light yellow crystalline product was filtered, washed with water, and dried in a desiccator at ambient temperature. The material was single phase, as judged by comparison of the powder X-ray diffraction of the bulk product to the pattern simulated from the coordinates derived from the single-crystal study. The yield was 85% based on iron. Increasing the reaction temperature to 200 °C led to decomposition of the amine template and the formation of spheniscidite, $NH_4[Fe_2(OH)(PO_4)_2] \cdot 2H_2O$.[13] The second compound, $[H_3N(CH_2)_3NH_3][Fe_2O(PO_4)_2]$, was prepared by hydrothermal treatment of $FeCl_3 \cdot 6H_2O$ (2.5 mmol), H_3PO_4 (7.5 mmol), 1,3-diaminopropane (14 mmol), *n*-butanol (7 mL), and water (3 mL) for 3 days at 165 °C and by cooling to room temperature at 5 °C/h. The amine content of the gel precursor was twice as much as that for the first compound, which led to a structure containing oxide anion and only PO_4 groups. The reaction product contained orange plate crystals of $[H_3N(CH_2)_3$-

$NH_3][Fe_2O(PO_4)_2]$ in a yield of 94% and a very small amount of a light yellow material, $[H_3N(CH_2)_3NH_3]_2[Fe_4(OH)_3(HPO_4)_2(PO_4)_3]\cdot xH_2O$. With water as the only solvent, there was a tendency to produce $[H_3N(CH_2)_3NH_3][Fe_2O(PO_4)_2]$ in low yield with a mixture of unidentified phases. Decreasing the amine content of the gel, which had an overall composition 1.5 $FeCl_3$:7.5 H_3PO_4:3.7 $H_2N(CH_2)_3NH_2$:555 H_2O, led to the formation of $FePO_4\cdot 2H_2O$.[14] The pH value, solvent, and reaction temperature, as indicated from the above description, affect the products formed in the reactions.

An alternative route using HF as the mineralizer was initiated by Ferey and co-workers. An interesting set of compounds labeled ULM-n were prepared, in which most of the materials have fluorine directly bonded to iron.[15] The usual starting pH of the reaction mixture was very acidic, in order to dissolve Fe_2O_3, which was often used as the source of iron. The use of HF produced a number of microporous frameworks which do not form in a fluoride-free medium. In view of the success of the synthesis of gallofluorophosphate phases using HF mineralizers,[16] it is likely that similar preparative methods should also be successful for iron fluorophosphates.

The remainder of this paper will present the structures and properties of the iron phosphate phases incorporating organic templates. The ULM-n materials prepared by Ferey and co-workers will not be discussed here. The discussion of the phosphates below will be organized according to the basis of connectivity: a few examples each of three-dimensional (3-D) framework, 2-D layered and 1-D chain structures. The compounds discussed in this paper are collected in Table 1. The synthesis conditions are summarized in Table 2.

Three-Dimensional Compounds

This class of FePOs is the most diverse and has the largest number of different structure types. The first FePO synthesized with a substantial micropore volume, $[H_3N(CH_2)_3NH_3]_2[Fe_4(OH)_3(HPO_4)_2(PO_4)_3]\cdot xH_2O$ with $x \sim 9$ (compound **1**), contains a tetrameric building unit as shown in Figure 1.[11] We have also found that the 3-D $[Fe_4(OH)_3(HPO_4)_2(PO_4)_3]^{4-}$ framework can accommodate diprotonated 1,4-diaminobutane cations.[17] The building unit consists of two central FeO_6 octahedra that share a common edge, with the two hydroxo oxygens involved in the shared edge serving as corners for two additional FeO_6 octahedra. The phosphate tetrahedra that complete the building unit are of three types: the first type of phosphate shares three corners with three octahedra within a tetramer with the remaining corner as a terminal hydroxy group; the second phosphate shares two corners with two octahedra within a tetramer and one corner with an octahedron in a different tetramer, with the remaining corner serving as H-bond acceptor from propylenediammonium cation and HPO_4 group; the third phosphate shares two corners with two octahedra within a tetramer and the other two corners with two octahedra in a different tetramer. A topologically identical cluster exists in the iron phosphate mineral leucophosphite, $K_2[Fe_4(OH)_2(H_2O)_2(PO_4)_4]\cdot 2H_2O$.[18] The terminal aquo ligand in leucophosphite is replaced by a doubly bridging OH group which connects adjacent tetramers via −Fe−OH−Fe− bonds forming orthogonal, but nonintersecting, infinite chains parallel to the ⟨100⟩ directions of the tetragonal cell of **1** (Figure 2). One may regard the infinite chain as a column. In a unit cell, there are four layers of columns with z values equal to 0, $^1/_4$, $^1/_2$, and $^3/_4$, respectively. Each column lies in an a-glide plane and columns in adjacent layers are 4_1-screw axis related. The columns are interlinked by phosphate tetrahedra generating large tunnels running parallel to ⟨100⟩, in which the diprotonated 1,3-diaminopropane and water molecules reside (Figure 3). The amines molecules are well-ordered, which can be attributed to the formation of hydrogen bonds. There are about nine H_2O of crystallization per formula unit according to TG and elemental analyses. However, only four lattice water sites in the structural tunnels could be located. Each site is partially occupied. Within tunnels there are 20-ring windows formed by the edges of 10 iron−oxygen octahedra and 10 phosphate tetrahedra in an alternating manner. The HPO_4 groups project into the tunnels at a nearest O−O distance of 7.35 Å. The long side of the ring has a free dimension (minimum O−O distance less one O diameter of 2.6 Å) of 10.4 Å. The angle between the least-squares plane

Table 1

no.	composition dimensionality	crystal data	ref
1	$[H_3N(CH_2)_3NH_3]_2[Fe_4(OH)_3(HPO_4)_2(PO_4)_3]\cdot H_2O$ 3-D	tetragonal, $I4_1/a$ $a = 15.3822(5)$ Å $c = 28.908(1)$ Å	11
2	$[H_3N(CH_2)_2NH_3]_2[Fe_4O(PO_4)_4]\cdot H_2O$ 3-D	monoclinic, $C2$ $a = 30.3801(5)$ Å $b = 10.1204(5)$ Å $c = 10.0977(5)$ Å $\beta = 107.712(1)°$	22
3	$(C_4H_{12}N_2)[Fe_4(OH)_2(HPO_4)_5]$ 3-D	monoclinic, $C2/m$ $a = 25.706(3)$ Å $b = 6.4492(6)$ Å $c = 6.3790(6)$ Å $\beta = 102.601(2)°$	30
4	$(C_4H_{12}N_2)_2[Fe_6(HPO_4)_2(PO_4)_6(H_2O)_2]\cdot H_2O$ 3-D	triclinic, $P\bar{1}$ $a = 9.1768(1)$ Å $b = 12.7229(1)$ Å $c = 16.4830(2)$ Å $\alpha = 68.530(1)°$ $\beta = 83.285(1)°$ $\gamma = 73.259(1)°$	31
5	$[HN(CH_2CH_2)_3NH][Fe_8(HPO_4)_{12}(PO_4)_2(H_2O)_6]$ 3-D	trigonal, $P\bar{3}c1$ $a = 13.5274(5)$ Å $c = 19.2645(6)$ Å	32
6	$[H_3N(CH_2)_2NH_3]_{0.5}[Fe(OH)(PO_4)]$ 2-D	monoclinic, $P2_1/c$ $a = 4.5010(7)$ Å $b = 6.114(1)$ Å $c = 18.460(3)$ Å $\beta = 94.59(1)°$	34, 35
7	$[H_3N(CH_2)_3NH_3][Fe_2O(PO_4)_2]$ 2-D	monoclinic, $P2_1/c$ $a = 11.6591(8)$ Å $b = 9.5718(7)$ Å $c = 10.1158(7)$ Å $\beta = 99.963(2)°$	12
8	$(C_4H_{11}N_2)_{0.5}[Fe_3(HPO_4)_2(PO_4)(H_2O)]$ 2-D	monoclinic, $C2/c$ $a = 30.8924(4)$ Å $b = 6.3733(1)$ Å $c = 12.5552(2)$ Å $\beta = 101.946(1)°$	30
9	$[trans-1,2-C_6H_{10}(NH_3)_2][Fe(OH)(HPO_4)_2]\cdot H_2O$ 1-D	orthorhombic, $Pbcm$ $a = 8.6644(2)$ Å $b = 21.7503(4)$ Å $c = 7.2626(2)$ Å	39
10	$(C_4H_{12}N_2)_{1.5}[Fe_2(OH)(H_2PO_4)(HPO_4)_2(PO_4)]\cdot 0.5H_2O$ 1-D	triclinic, $P\bar{1}$ $a = 6.3347(2)$ Å $b = 13.0075(4)$ Å $c = 13.7810(1)$ Å $\alpha = 62.834(1)°$ $\beta = 81.404(1)°$ $\gamma = 82.688(1)°$	42

Table 2. Summary of Synthesis Conditions

no.	reactant gel composition (mmol)[a]	temp, °C	product
1	1.5 $FeCl_3 \cdot 6H_2O$, 7.5 H_3PO_4, 7.5 1,3-diaminopropane, 555 H_2O	165	yellow crystals
2	2 $FeCl_2 \cdot 4H_2O$, 2 $FeCl_3 \cdot 6H_2O$, 7.2 H_3PO_4, 12 ethylenediamine, 500 H_2O	175	dark-brown crystals
3	2.5 $FeCl_3 \cdot 6H_2O$, 11 H_3PO_4, 7.5 piperazine, 500 H_2O	180	yellow crystals
4	1 $FeCl_2 \cdot 4H_2O$, 1 $FeCl_3 \cdot 6H_2O$, 13 H_3PO_4, 6 piperazine, 250 H_2O, 80 EG	180	brown crystals
5	2.5 $FeCl_3 \cdot 6H_2O$, 7.5 H_3PO_4, 7.5 DABCO, 389 H_2O, 33 *n*-butanol	180	colorless crystals + green unidentified phase
6	1.66 $FeCl_3 \cdot 6H_2O$, 5.98 H_3PO_4, 6.97 ethylenediamine, 444 H_2O	160	greenish-yellow crystals
7	2.5 $FeCl_3 \cdot 6H_2O$, 7.5 H_3PO_4, 14 1,3-diaminopropane, 167 H_2O, 76 *n*-butanol	160	orange crystals + yellow PX (**1**)
8	0.5 $FeCl_3 \cdot 6H_2O$, 1.5 $FeCl_2 \cdot 4H_2O$, 6 H_3PO_4, 6 piperazine, 250 H_2O, 80 EG	180	dark green crystals + brown PX (**4**)
9	1 $FeCl_3 \cdot 6H_2O$, 7.5 H_3PO_4, 7.5 *trans*-1,2-diaminocyclohexane, 555 H_2O	120	colorless crystals
10	1 $FeCl_3 \cdot 6H_2O$, 6 H_3PO_4, 6 piperazine, 250 H_2O, 80 EG	110	colorless PX

[a] EG = ethylene glycol, DABCO = 1,4-diazabicyclo[2.2.2]octane, PX = polycrystalline powder.

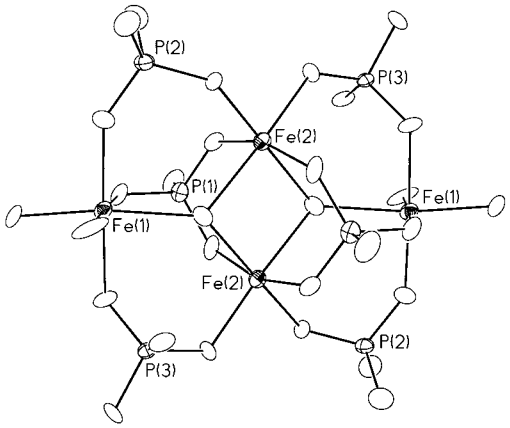

Figure 1. The tetranuclear iron cluster in **1**. Unless otherwise noted, thermal ellipsoids are shown at 60% probability. Filled lines and single lines are for Fe−O and P−O bonds, respectively.

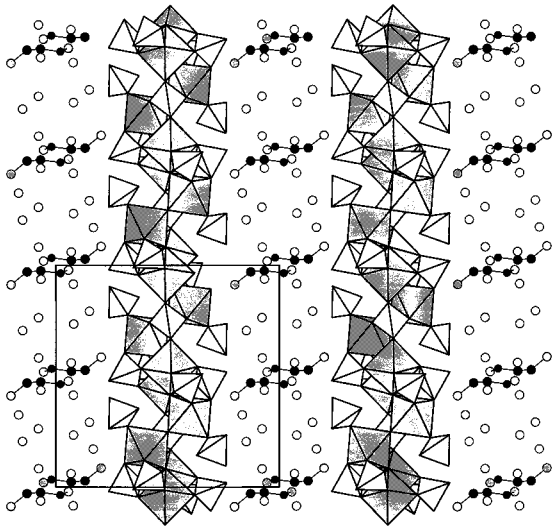

Figure 2. Parallel infinite chains in **1** formed of tetranuclear iron clusters and phosphate tetrahedra. In this presentation, the corners of octahedra and tetrahedra are oxygen atoms and the iron and phosphorus are at the centers of each octahedron and tetrahedron, respectively. Unless otherwise noted C, N, and water oxygen atoms are represenated by solid, stippled, and open circles, respectively.

of the 20-ring and the *ab*-plane is 55°. The framework also contains a large cavity with a local symmetry of S_4 formed by four 20-rings, through which they communicate orthogonal, nonintersecting tunnels (Figure 4). The presence of the large cavities is also reflected in the very low framework metal atom density. For **1**, there are 10.5 M atoms (M = Fe, P) per 1000 Å^3, compared with the value of 12.7 atoms for the very open

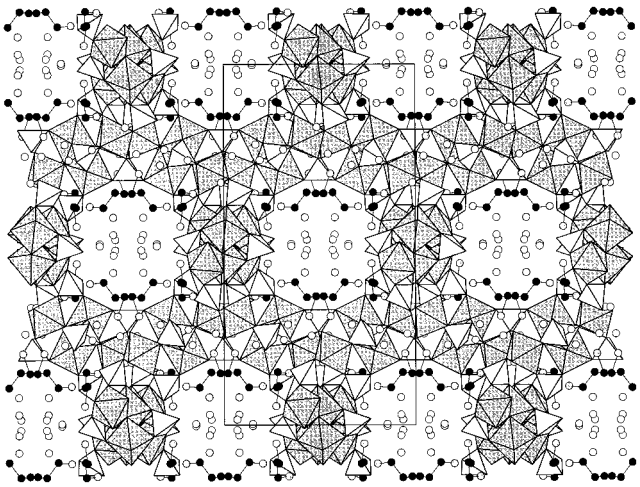

Figure 3. Structure of **1** viewed along the [010] direction.

faujasite (M = Si),[19] 12.1 atoms (M = Fe, P) for the phosphate mineral cacoxenite, which contains enormous channels,[2] and 9.3 atoms for $[HN(CH_2CH_2)_3NH]K_{1.35}[V_5O_9(PO_4)_2] \cdot xH_2O$ (M = V, P), which is among the lowest framework density materials known.[8]

Strictly speaking, a material is only a molecular sieve when the templates can be removed from the channels. The framework of **1** collapses at about 150 °C in air, as is indicated from powder X-ray diffraction. However, the large template $[H_3N(CH_2)_3NH_3]^{2+}$ can be ion-exchanged with the smaller cation NH_4^+ to leave room in the channels. Stirring **1** with a concentrated aqueous solution of ammonium chloride at 50 °C overnight results in ion exchange of 83% of the organic template according to TG and elemental analyses. The thermal stability of the ion-exchanged product is not improved. The gallium and indium analogues of **1** were also synthesized under similar reaction conditions by using the organic template 1,4-diaminobutane and $Ga(NO_3)_3 \cdot 6H_2O$ and $In(NO_3)_3 \cdot 6H_2O$ as the sources for Ga and In.[20] Powder X-ray diffraction indicates that they are isostructural. The In compound was also characterized by single-crystal X-ray diffraction. Topological analogue of the tetrameric iron−oxygen cluster in **1** also occurs in $NH_4[Ga_2(PO_4)_2(OH)(H_2O)] \cdot H_2O$.[21] However, the tetrameric indium−oxygen cluster is observed for the first time. The very open framework of **1** should allow the encapsulation of metal complexes. Further research in this aspect is in progress.

Another 3-D FePO built up from tetranuclear moieties is the mixed-valence iron phosphate $[H_3N(CH_2)_3NH_3]_2[Fe_4O(PO_4)_4] \cdot H_2O$ (**2**).[22] It is the first mixed-valence iron

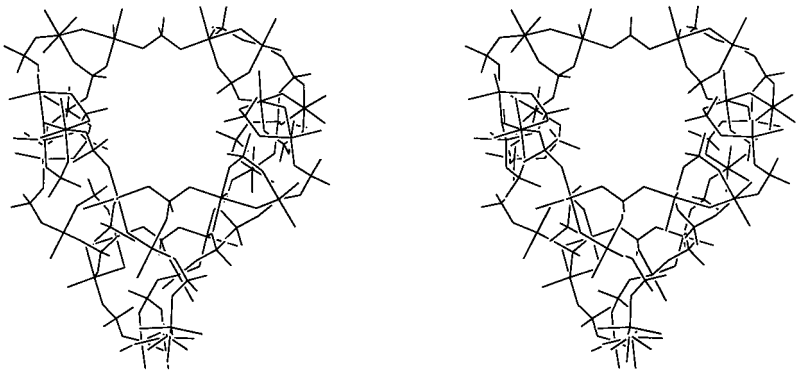

Figure 4. Stereo line drawing of the large cavity in **1** formed of four 20-rings. Each ring consists of 10 iron−oxygen octahedra and 10 phosphate tetrahedra in an alternating manner.

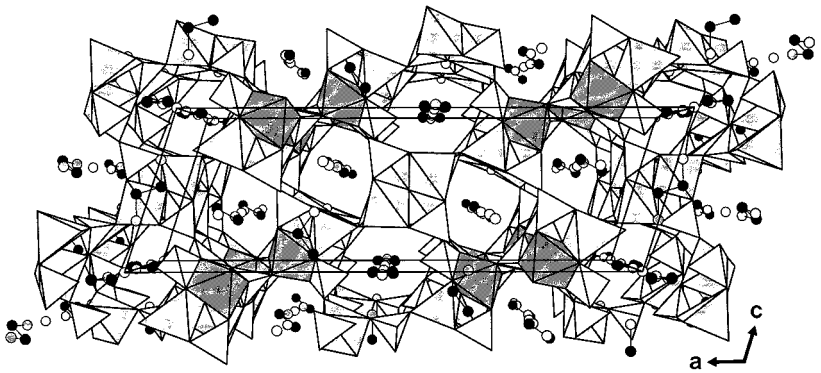

Figure 5. Perspective view of the structure of **2** along [010]. Polyhedra with darker and lighter shades are FeO_6 octahedra and FeO_5 trigonal bipyramids, respectively.

phosphate with a 3-D framework structure containing organic templates. There does, however, exist a bidimensional mixed-valence iron fluorophosphate with intercalated ethylenediammonium cation.[23] Microporous mixed-valence iron phosphate is of interest from the viewpoint of catalysis, because the more active and selective phase in the industrial iron phosphate catalyst is a mixed-valence compound.[24]

Monophasic **2** was prepared by reaction of $FeCl_3 \cdot 6H_2O$ (2 mmol), $FeCl_2 \cdot 4H_2O$ (2 mmol), H_3PO_4 (7.2 mmol), $H_2N(CH_2)_2NH_2$ (12 mmol), and water (9 mL) for 3 d at 175 °C. The compound crystallizes in the monoclinic space group *C*2 with a cell volume of 2957.5(4) Å^3. It adopts a novel structure with an open framework. Figure 5 shows the structure viewed along the [010] direction. The asymmetric unit contains two types of tetranuclear Fe−O clusters linked via oxygen to phosphate tetrahedra to form the building units of the framework. As shown in Figure 6a, one type of cluster has a μ_4-oxygen atom at the center of the Fe_4 tetrahedron; each Fe has a trigonal bipyramidal configuration with an apical oxygen as the common vertex. The PO_4 tetrahedron shares three corners with three Fe atoms within a cluster with the fourth corner being coordinated to an Fe atom of an adjacent cluster. Valence sum calculation shows that Fe(3) is trivalent and Fe(5) is divalent. Alternatively, the cluster has a cubane-type structure with an Fe_4P_4 cube surrounding a central μ_4-oxygen with the bridging oxygen approximately on each edge of the cube. The cubane-type O-centered Fe_4P_4 cluster is observed for the first time in phosphates. However, this topology is already known in fluorinated open framework structures with fluorine in the center of octamer. The examples are cloverite,[25] octadecasil,[26]

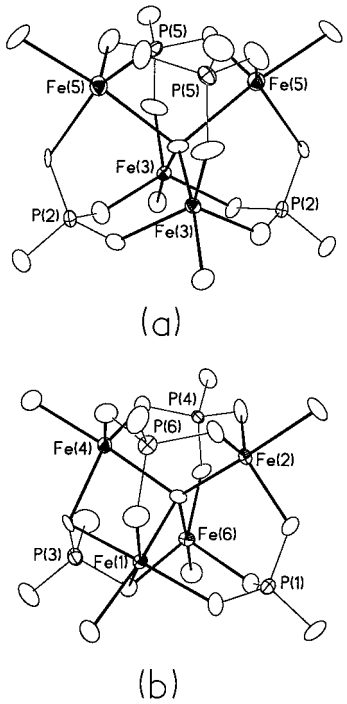

Figure 6. Two types of tetranuclear iron−oxygen cluster in **2**. (a) Cluster with four trigonal bipyramidal iron atoms and (b) cluster with one octahedral iron and three trigonal bipyramidal iron atoms.

and ULM-5.[27] An analogous structural skeleton is also found in the tetranuclear copper complexes with the general formula $[Cu_4OX_6L_4]$, where X is a bridging halogen and L an axially bonded unidentate ligand.[28] The second type of Fe_4P_4 cubane-like cluster contains three FeO_5 trigonal bipyramids and one FeO_6 octahe-

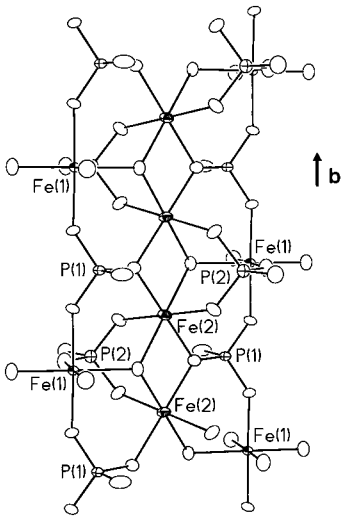

Figure 7. Section of a layer in **3** showing two types of chains running parallel to the *b*-axis.

dron (Figure 6b). The $Fe(1)O_6$ octahedron shares two skew edges with two FeO_5 trigonal bipyramids. A phosphate tetrahedron shares an edge with $Fe(1)O_6$. The two oxygen atoms forming the shared edge further coordinate to two Fe atoms. Fe(1) and Fe(2) are trivalent and the other two Fe atoms are divalent. Octahedral Fe(1) is trivalent, although high-spin Fe^{2+} gains slightly more crystal field stabilization energy by going into an octahedral site than by occupying a trigonal bipyramidal site. The clusters are connected via Fe−O−P bonds to form intersecting eight-membered channels parallel to the [010] and [001] directions, where the ethylenediammonium cations and water molecules reside. The water molecules are located at the intersections of these channels.

Recently, DeBord et al. reported the synthesis and characterization of compound **2**.[29] It was prepared in very low yield (∼1%) from the hydrothermal treatment of Fe_2O_3, H_3PO_4, ethylenediamine, HF, and H_2O at 200 °C. The structure determination was based on the tetragonal space group $I\bar{4}2m$ with a cell volume of 989.6(1) Å^3, which is one-third of the volume of the monoclinic cell reported by us. Interestingly, the structure consists of only one type of cubane-like cluster formed of four trigonal bipyramidal iron and four tetrahedral phosphorus atoms. The carbon atoms of the ethylenediammonium cation were found to be 2-fold disordered. Presumably the structure determination was based on a subcell.

Another mixed-valence FePO, $(C_4H_{12}N_2)[Fe_4(OH)_2(HPO_4)_5]$ (**3**),[30] with a new framework topology, was prepared as a monophasic product from a gel solution of $FeCl_3{\cdot}6H_2O$, $FeCl_2{\cdot}4H_2O$, H_3PO_4, piperazine, ethylene glycol, and water. The framework contains two types of chains, running along the [010] direction (Figure 7). The first type of chain, with the formulation $[FeO_4]_\infty$, is built up from trans-edge-sharing $Fe^{II}O_6$ octahedra. The second one, denoted as $[FePO_8]_\infty$, is formed of alternating and corner-sharing $Fe^{III}O_6$ octahedra and HPO_4 groups. The preference of Fe^{II} ions for the sites in $[FeO_4]_\infty$ can be rationalized by a smaller $Fe^{II}-Fe^{II}$ repulsion in the edge-sharing octahedra. The two types of chains are connected in such a way that $Fe^{II}O_6$ octahedra of one $[FeO_4]_\infty$ chain share corners with $Fe^{III}O_6$ octahedra and HPO_4 groups of two $[FePO_8]_\infty$ chains. This arrangement forms a $[Fe_4P_2O_{20}]_\infty$ ribbon constituted by three chains. The ribbons are linked by HPO_4 groups to form slabs parallel to the *bc*-plane with the formulation $[Fe_4P_4O_{20}]_\infty$, which are further connected by HPO_4 tetrahedra via corner-sharing with the $Fe^{III}O_6$ octahedra, generating a 3-D framework with intersecting 8-ring channels parallel to the [001] and [010] directions (Figure 8). Diprotonated piperazinium cations, which are disordered over two sites, reside at the intersections of these channels. Empty 6-ring channels parallel to [010] are also formed within the slabs.

The piperazine encapsulating iron(III) compound $(C_4H_{12}N_2)_2[Fe_6(HPO_4)_2(PO_4)_6(H_2O)_2]{\cdot}H_2O$ (**4**) is formed of layers of iron phosphate which are connected by FeO_5 trigonal bipyramids and HPO_4 groups to form a 3-D framework structure (Figure 9).[31] Each layer contains dimers of corner-sharing FeO_6 octahedra connected by PO_4 tetrahedra via corner- or edge-sharing. The framework contains 1-D channels with eight-sided windows, in which the charge-compensating diprotonated piperazinium cations are located.

$[HN(CH_2CH_2)_3NH]_3[Fe_8(HPO_4)_{12}(PO_4)_2(H_2O)_6]$ (**5**),[32] which crystallizes in the trigonal space group $P\bar{3}c1$, consists of layers of corner-sharing FeO_6 and $FeO_5(OH_2)$ octahedra and PO_4 and $PO_3(OH)$ tetrahedra bonded together by additional FeO_6 octahedra to form a two-dimensional array of intersecting channels parallel to the ⟨100⟩ directions of a trigonal unit cell in which the charge-compensating diprotonated 1,4-diazabicyclo[2.2.2]octane (DABCO) cations reside (Figure 10). Within the channels are 14-membered rings formed by seven iron−oxygen octahedra and seven phosphate tetrahedra. The framework is closely related to that of an imidazole-encapsulating indium phosphate, $[H_3O][C_3N_2H_5]_3[In_8(HPO_4)_{14}(H_2O)_6]{\cdot}5H_2O$.[33]

Two-Dimensional Layered Materials

There are several examples of layered FePOs. Compound **6**, $[H_3NCH_2CH_2NH_3]_{0.5}[Fe(OH)(PO_4)]$, which was synthesized from hydrothermal reactions in water by Cavellec et al. and DeBord et al.,[34,35] consists of infinite chains of edge-sharing FeO_6 octahedra linked into 2-D sheets by PO_4 tetrahedra that possess terminal P═O groups which protrude into the interlamellar space. The projection of P═O also serves to provide distinct channels, occupied by ethylenediammonium cations. The cations contact both adjacent layers via a hydrogen-bonded network. The structure is isotypic with the layered gallophosphate synthesized in ethylene glycol by Jones et al.[36]

The iron(III) phosphate **7**, $[H_3N(CH_2)_3NH_3][Fe_2O(PO_4)_2]$,[12] crystallizes in a unique structure type containing novel tetramers of FeO_5 trigonal bipyramids. The compound was synthesized using a mixture of *n*-butanol and water as a solvent. The structure consists of anionic sheets of iron phosphate in the *bc*-plane with charge-compensating propanediammonium cations between the sheets (Figure 11). The sheets are constructed from tetramers of FeO_5 trigonal bipyramids, which are joined to four other tetramers by the bridging phosphate ligands as shown in Figure 12. Each sheet has a double-layered structure. Within a layer, FeO_5

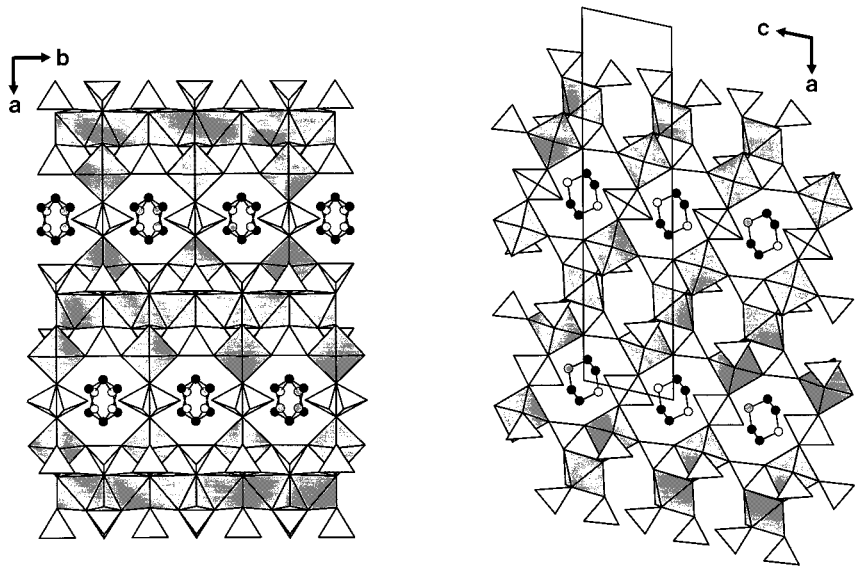

Figure 8. Structure of **3** viewed along (left) [001] and (right) [010]. The carbon atoms of piperazinium cations and the phosphate group which connects adjacent layers are disordered.

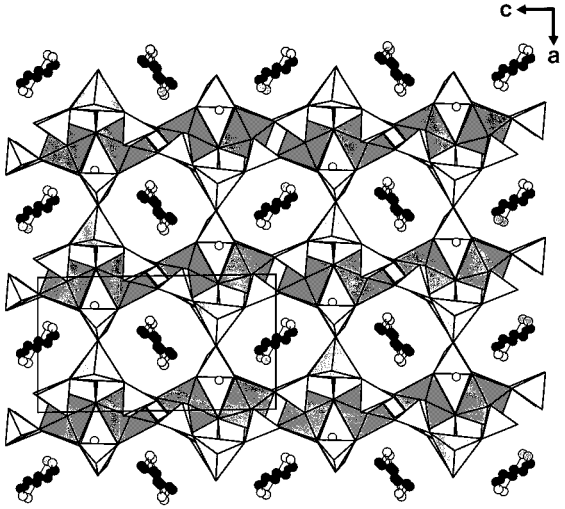

Figure 9. Structure of **4** viewed along [010]. Polyhedra with darker and lighter shade are FeO_6 octahedra and FeO_5 trigonal bipyramids, respectively.

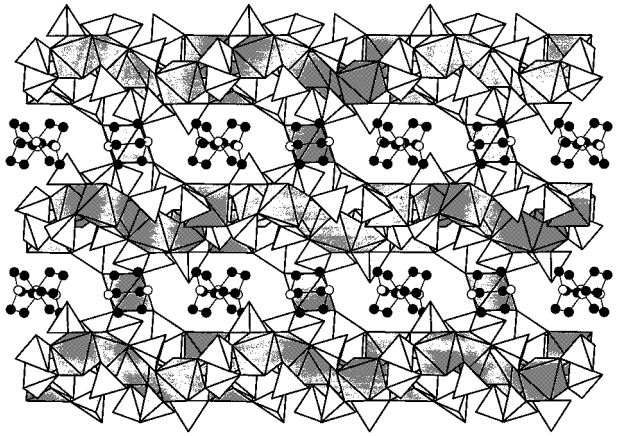

Figure 10. Structure of **5** viewed along [100] of a trigonal cell.

trigonal bipyramids share corners with PO_4 tetrahedra in alternating manner to form eight-sided windows. Infinite tunnels are formed along the [100] direction, in which the organic molecules are located. The molecules are locked in their positions by hydrogen bonds to phosphate oxygens. The tetramer contains a dimer of edge-sharing trigonal bipyramids which further links at the shared corners to two other trigonal bipyramids forming an Fe_4O_{16} cluster (Figure 13). The tetramer possesses *Ci* symmetry located at the midpoint of the shared edge. One phosphate oxygen is present as a pendant P═O unit and projects into the interlamellar region. The most remarkable structural feature of **7** is the presence of a novel Fe_4O_{16} cluster formed of four FeO_5 trigonal bipyramids. Although five-coordination with trigonal bipyramidal geometry is frequently found in iron phosphates, iron−oxygen clusters formed of only FeO_5 trigonal bipyramids are very rare. To our knowledge, Fe_3PO_7[37] and $[H_3N(CH_2)_3NH_3]_2Fe_4O(PO_4)_4 \cdot H_2O$[22,29] are the only other iron phosphates which contain clusters of FeO_5 trigonal bipyramids. However, topologically identical tetramers of trigonal bipyramids also occur in $AlPO_4$-12 and $GaPO_4$-12.[38]

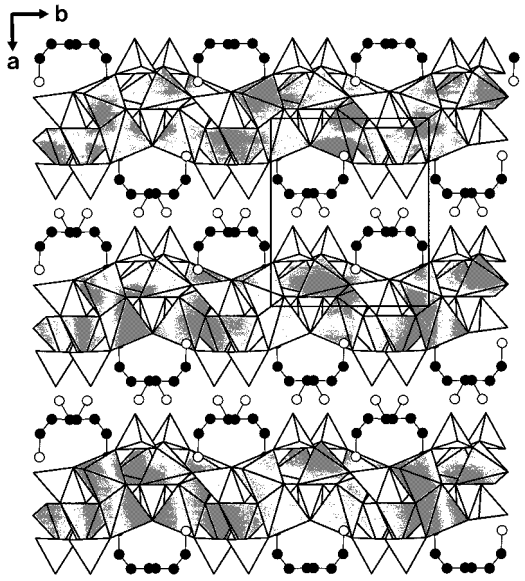

Figure 11. Structure of **7** viewed along [001]. Polyhedral with darker shade, FeO_5 trigonal bipyramids; tetrahedra with lighter shade, PO_4.

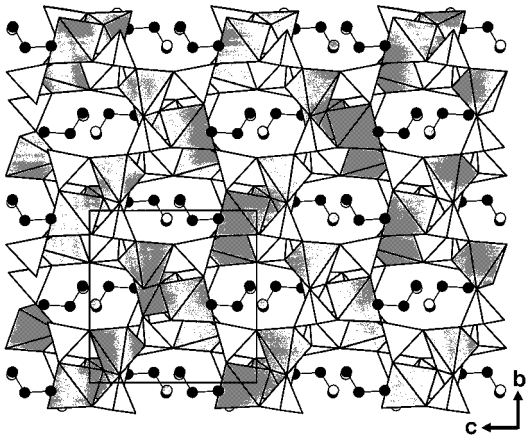

Figure 12. Section of a sheet in **7** showing the connectivity between the iron−oxygen clusters.

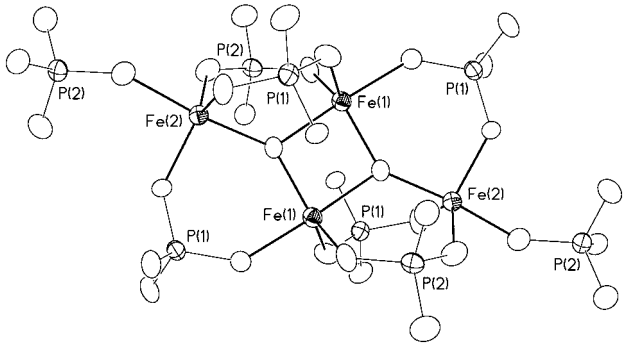

Figure 13. The tetranuclear iron−oxygen cluster in **7**.

Another 2-D FePO built up from novel iron−oxygen clusters is the mixed-valence phosphate $(C_4H_{11}N_2)_{0.5}$-$[Fe_3(HPO_4)_2(PO_4)(H_2O)]$ (**8**).[30] It was synthesized from a gel solution of $FeCl_3 \cdot 6H_2O$, $FeCl_2 \cdot 4H_2O$, H_3PO_4, piperazine, ethylene glycol, and water, which, as compared with that for compound **3**, contains less H_3PO_4. A mixture of ethylene glycol and water produces a reducing environment because both **3** and **8** were also obtained even when only $FeCl_3 \cdot 6H_2O$ was used in the reaction mixture. Compound **8** has a layered structure with monoprotonated piperazinium cations in the interlayer space (Figure 14). The basic building unit of each layer is a hexamer which is composed of two FeO_6 octahedra and four FeO_5 trigonal bipyramids (Figure 15). All of these iron−oxygen polyhedra are connected via edge-sharing. The core of the hexamer is a dimer of FeO_6 octahedra, each of which shares its two skew edges with FeO_5 trigonal bipyramids. These hexamers are connected into 2-D layers by phosphate tetrahedra and Fe−O−Fe bonds. Bond-valence calculations indicate that both trigonal bipyramidal iron atoms are divalent, and the octahedral iron has a valence sum of 2.5. This compound is the most Fe^{II} rich of the organically templated FePO frameworks. The electric field gradient calculations based on the room-temperature Mossbauer measurements confirm the presence of mixed-valence iron at the octahedral site and the trigonal bipyramidal sites as pure Fe^{II}. Furthermore, the relative peak area of Fe^{III} is in agreement with the result of bond-valence calculations.

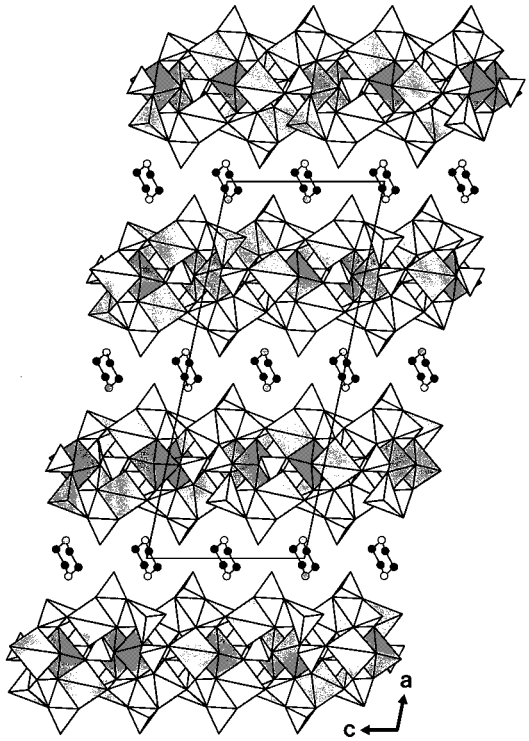

Figure 14. Structure of **8** viewed along [010]. Polyhedra with darker and lighter shade are FeO_6 octahedra and FeO_5 trigonal bipyramids, respectively.

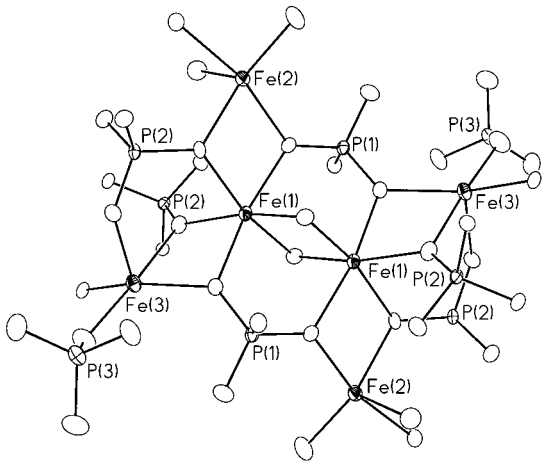

Figure 15. Section of a layer in **8**.

One-Dimensional Chain Structures

Phosphate $[(1R,2R)\text{-}C_6H_{10}(NH_2)_2][Fe(OH)(HPO_4)_2] \cdot H_2O$ is an interesting FePO because of the incorporation of a chiral amine. On the basis of powder X-ray diffraction, it is isostructural with the Ga compound $[(1R,2R)\text{-}C_6H_{10}(NH_2)_2][Ga(OH)(HPO_4)_2] \cdot H_2O$,[39] which has been characterized by single-crystal X-ray diffraction. In the case of the Fe compound, it is difficult to obtain single crystals that are suitable for structural analysis. Its composition was defined by TG and elemental analyses. The structure of the Ga compound is shown in Figure 16. It crystallizes in the enantiomorphic space group $P2_1$ with $a = 8.7208(2)$ Å, $b = 7.1276(2)$ Å, $c = 11.1411(4)$ Å, and $\beta = 96.129(1)°$. It consists of infinite chains of trans-corner-sharing $GaO_5(OH)$ octahedra (Figure 17). The central axis of each chain is a 2_1-screw axis. The metal atoms are linked together by means of

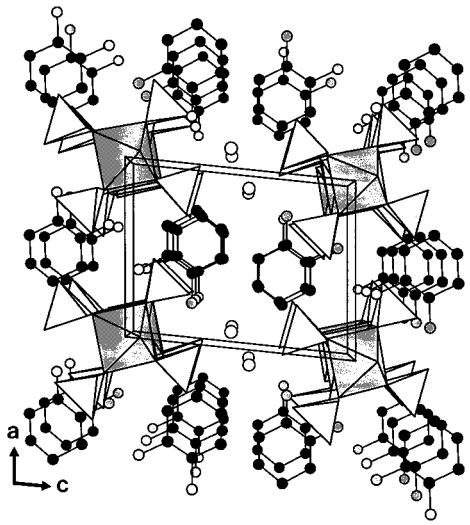

Figure 16. The $[(1R,2R)\text{-}C_6H_{10}(NH_3)_2][Ga(OH)(HPO_4)_2]\cdot H_2O$ structure viewed along [010].

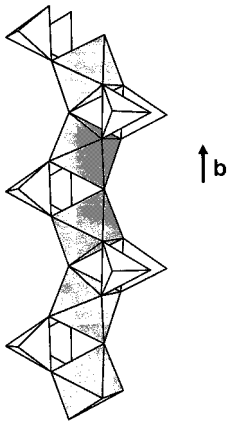

Figure 17. Section of an infinite chain in $[(1R,2R)\text{-}C_6H_{10}(NH_3)_2][Ga(OH)(HPO_4)_2]\cdot H_2O$, viewed in a direction perpendicular to [010].

single bridges of hydroxo groups to produce a zigzag Ga−O(H)−Ga−O(H) backbone with alternating short and long Ga−O(H) bonds (1.967, 2.007 Å). Adjacent octahedra within a chain are bridged by phosphate groups in the same manner as those in $Na_3M(OH)(HPO_4)(PO_4)$ (M = Al, Ga)[40] and in $[M(TO_4)_2\phi]$ chains (T, 4-coordinate cation; ϕ, unspecified anion ligand) of phosphate, sulfate, and silicate minerals.[41] The organic cation is nested via a hydrogen-bonded network. An alternation of the Al−O bond length (1.930, 1.946 Å) along the chain axis is also present in the mineral overite, $CaMgAl(OH)(PO_4)_2(H_2O)_4$, although it crystallizes in a centrosymmetric space group.[42] Therefore, such bond alternation does not necessarily result from the presence of a chiral template. In the case of $[(1R,2R)\text{-}C_6H_{10}(NH_2)_2][Ga(OH)(HPO_4)_2]\cdot H_2O$, the degree to which the chirality of the template is transferred to the lattice appears small. For comparison, the iron phosphate containing racemic *trans*-1,2-diaminocyclohexane was synthesized and structurally characterized by single-crystal X-ray diffraction. $[trans\text{-}1,2\text{-}C_6H_{10}(NH_3)_2][Fe(OH)(HPO_4)_2]\cdot H_2O$ (**9**) crystallizes in the centrosymmetric, orthorhombic space group *Pbcm*. The structure consists of $[M(TO_4)_2\phi]$ chains which are topologically identical to those in the chiral compound. However, each chain sits on a 2-fold screw axis with a

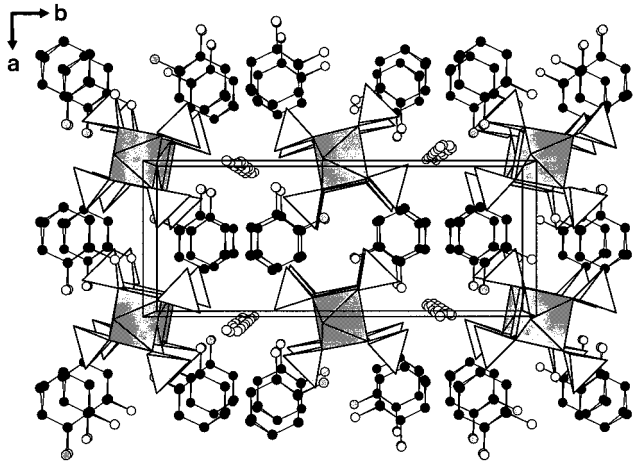

Figure 18. Structure of **9** viewed along [001].

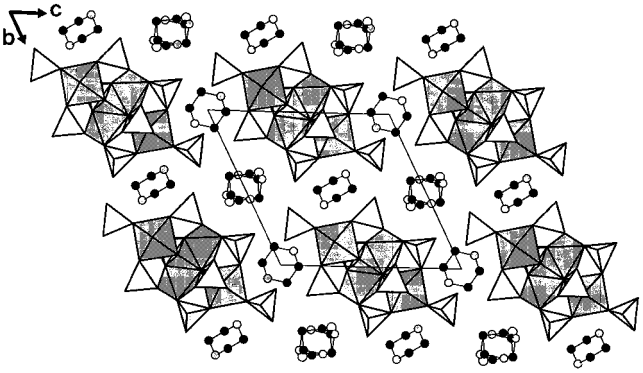

Figure 19. Structure of **10** viewed along [100]. The piperazine molecule, which is centered at $(0,{}^1/_2,0)$, is disordered over two positions.

center of symmetry with equal Fe−O bond length along the Fe−O(H)−Fe−O(H) backbone. As shown in Figure 18, the $[trans\text{-}1,2\text{-}C_6H_{10}(NH_3)_2]^{2+}$ cations are arranged in a way different from that in the chiral structure. There is also extensive hydrogen bonding between the phosphate oxygens, amine groups of the cation, and the lattice water. There is probably a direct relationship between the arrangement of the hydrogen bonding groups on the organic cations and the topology of the structure.

$(C_4H_{12}N_2)_{1.5}[Fe_2(OH)(H_2PO_4)(HPO_4)_2(PO_4)]\cdot 0.5H_2O$ (**10**) is another example of 1-D FePO.[43] As shown in Figure 19, the structure consists of infinite chains of iron phosphate, which are H-bonded with amine groups of piperazinium dications. Each chain is built up from a tetranuclear Fe_4O_{20} cluster which is topologically identical with those in the mineral leucophosphite and compound **1**. These tetranuclear clusters are connected into the 1-D chain by PO_4 tetrahedra and have terminal H_2PO_4 and HPO_4 groups (Figure 20). This is an unusual material in that it is the only example of 1-D FePO which is formed of iron−oxygen clusters. The molecule piperazine is a versatile agent which directs the formation of 3-D framework, 2-D layered, and 1-D chain structures such as compounds **3**, **4**, **8**, and **10**, respectively.

Conclusions and Future Possibilities

We have synthesized a number of iron phosphates incorporating organic amines in their structures. The

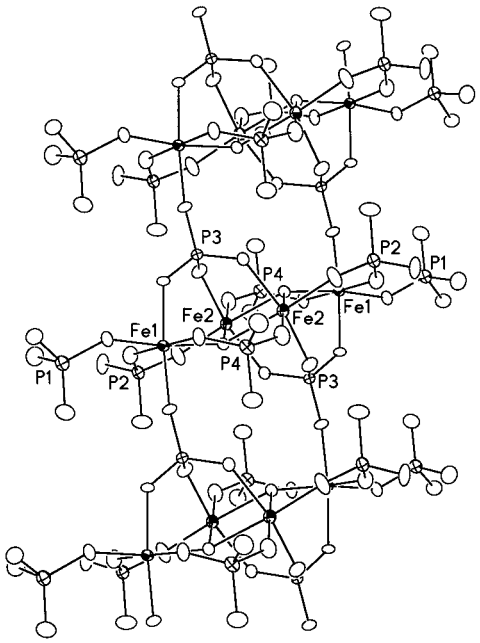

Figure 20. Section of the infinite chain in **10** showing the connectivity between tetranuclear clusters.

compositions of the prepared compounds are affected by the pH values of the reaction mixtures. For instance, compounds **2** and **7** contain oxo anions and only PO_4 groups because they were prepared from alkaline gels. Compound **1**, which contains both hydroxo anions and HPO_4 groups, was from a reaction mixture with an initial pH value of 6. Compound **8** was prepared from a gel with less H_3PO_4, as compared with compound **3**. Therefore, **8** contains a monoprotonated diamine template and a smaller amount of HPO_4. The choice of organic amines also has a strong influence on the structures of these materials. For example, compounds **1** and **5** adopt two very different structures, although the diamine/H_3PO_4 molar ratios in the reaction mixtures are the same.

It appears that 3-D FePO frameworks are the most diverse and 1-D infinite chain structures are the least common. This type of trend makes sense in terms of bond-valence theory. For P^{5+}, every oxide ligand receives a bond-valence contribution of 1.25 vu from the central cation, leaving 0.75 vu to be supplied by the rest of the structures. Thus most of the phosphates are highly polymerized, being dominated by frameworks and sheets, irrespective of any other variables (octahedral cation type, pH, temperature, pressure) that may also influence the stoichiometry and structure.[44] For silicates, only highly polymerized structures result.

Unlike the majority of previous reported FePOs with metal cation templates, these phosphates all contain relatively larger voids in the structures. The synthesis of large pores may be through the use of large organic templates or from gel precursors that already contain polynuclear iron−oxygen species. Although FePO frameworks with large cavities and windows have been prepared, they decompose upon attempts to remove incorporated organic cations from their void spaces. For example, the framework of $[H_3N(CH_2)_3NH_3]_2[Fe_4(OH)_3(HPO_4)_2(PO_4)_3]\cdot xH_2O$ (**1**) decomposes at about 150 °C in air. Therefore, the practical value of these materials is limited by their poor thermal stability compared to zeolites. This is not surprising in view of the fact that most the iron phosphates have the following structural features: terminal P−OH groups and other nontetrahedral framework groups (e.g., OH, H_2O). Additionally, if the strength of the interaction between template and framework increases, it might become even more difficult for these materials to be calcined to remove the templates. The large template may be ion-exchanged with small cations such as NH_4^+ to leave room in the channels, as observed from the ion-exchange property of $[H_3N(CH_2)_3NH_3]_2[Fe_4(OH)_3(HPO_4)_2(PO_4)_3]\cdot xH_2O$. These iron phosphate materials cannot be used at high temperature. However, they may find use for low temperature (and most probably liquid phase) applications.

The synthesis of chiral microporous materials is of great interest from the viewpoint of asymmetric catalysis. Although several chiral AlPOs and GaPOs prepared by using optically pure *d*-$Co(en)_3^{3+}$ as a structure-directing agent were reported,[45,46] the synthesis of microporous metal phosphates templated with chiral amines has not been successful. $[(1R,2R)\text{-}C_6H_{10}(NH_2)_2]\text{-}[Fe(OH)(HPO_4)_2]\cdot H_2O$ and the Ga analogue are the first metal phosphates containing a chiral amine. But they adopt a one-dimensional chain structure and it is unlikely that the amine can be removed without collapse of the structure. However, we believe that the use of chiral amines as structure-directing agents is a feasible route to prepare chiral open framework materials, which will be useful if the chirality remains when the templates are removed. We are continuing the exploratory synthesis of new metal phosphate frameworks with chiral templating agents.

Iron oxides have a rich structural chemistry. A large number of iron−oxygen clusters have been characterized. The organically templated iron phosphates greatly expand the variety of structures of iron−oxygen clusters. The tetranuclear clusters appear most versatile. The topological analogue of the Fe_4O_{20} cluster in leucophosphite also occurs in **1** and **10**. Tetramers of oxo-bridged trigonal bipyramids instead of octahedra are found in **7**. Hitherto unknown Fe_4P_4 cubane-type clusters formed of trigonal bipyramidal or octahedral iron and tetrahedral phosphorus atoms with a μ_4-oxygen at the center of each cube are shown to exist in **2**. These synthetic clusters may shed light on the structures of soluble aggregates during the condensation of hydrolyzed iron ions.

The incorporation of divalent transition metal into open-framework AlPO and GaPO (thereby forming MeAlPO and MeGaPO) are of interest because divalent metal not only confers Brønsted acidity upon the resulting solid but also introduces redox behavior.[47,48] Many examples of MeAlPOs and MeGaPOs have been reported.[49,50] Most of them adopt zeolite-type structures which are constructed from alternating PO_4 and MO_4 tetrahedra, where M is a disordered mixture of Al (or Ga) and a transition metal. However, $(C_6N_2H_{14})[MnGa(HPO_4)_2(PO_4)]$, which contains Mn^{2+} ions in distorted square-pyramidal geometry, has a new framework topology.[51] Since tetrahedral Fe^{2+} is very rare in phosphates and Fe^{2+} gains more crystal field stabilization energy at an octahedral site than at a tetrahedral site, iron(II)-substituted AlPOs and GaPOs may have

frameworks unlike any of those zeolite-type structures. On the basis of a large variety of framework architectures displayed by unsubstituted AlPOs and GaPOs, it is likely that many novel FeAlPO and FeGaPO structures can exist.

The synthesis of organically templated iron phosphates in aqueous or nonaqueous solvents is an exciting and promising field. Although we and others can now prepare crystalline pure phases of FePOs, we are still far away from being able to design and synthesize materials by demand. The major problems are the large number of synthetic variables, limited knowledge of the identity of cluster anions present in liquid phase, and poor understanding of the pathways, kinetics, and mechanisms of sol−gel reactions. The removal of the organic template without framework collapse is another problem. However, we are making progress in this area by synthesizing additional examples to obtain a better understanding of the factors influencing the synthesis and structures of these materials.

Acknowledgment. We thank the Institute of Chemistry, Academia Sinica and National Science Council of Taiwan for financial support and Professor T. -Y. Dong at National Sun-Yat Sen University, Taiwan and Dr. Nihn Nguyen at Laboratoire CRISMAT-ISMRA, Caen, France for Mossbauer spectroscopy measurements.

References

(1) Moore, P. B. *Am. Mineral.* **1970**, *55*, 135.
(2) Moore, P. B.; Shen, J. *Nature* **1983**, *306*, 356.
(3) Gleitzer, C. *Eur. J. Solid State Inorg. Chem.* **1991**, *28*, 77 and references therein.
(4) Lii, K.-H. *J. Chem. Soc., Dalton Trans.* **1996**, 819 and references therein.
(5) Bonnet, P.; Millet, J. M. M.; Leclercq, C.; Vedrine, J. C. *J. Catal.* **1996**, *158*, 128.
(6) Ai, M.; Muneyama, E.; Kunishige, A.; Ohdan, K. *J. Catal.* **1993**, *144*, 632.
(7) Haushalter, R. C.; Mundi, L. A. *Chem. Mater.* **1992**, *4*, 31 and references therein.
(8) Khan, M. I.; Meyer, L. M.; Haushalter, R. C.; Schweitzer, A. L.; Zubieta, J.; Dye, J. L. *Chem. Mater.* **1996**, *8*, 43 and references therein.
(9) Morris, R. E.; Weigel, S. J. *Chem. Soc. Rev.* **1997**, *26*, 309.
(10) Richens, D. T. *The Chemistry of Aqua Ions*; John Wiley & Sons: West Sussex, England, 1997.
(11) Lii, K.-H.; Huang, Y.-F. *J. Chem. Soc. Chem. Commun.* **1997**, 839.
(12) Lii, K.-H.; Huang, Y.-F. *J. Chem. Soc. Chem. Commun.* **1997**, 1311.
(13) Cavellec, M.; Riou, D.; Ferey, G. *Acta Crystallogr.* **1994**, *C50*, 1379.
(14) $FePO_4 \cdot 2H_2O$, file number 33-666; Joint Committee on Powder Diffraction Standards, International Center of Diffraction Data, Swarthmore, PA.
(15) Cavellec, M.; Riou, D.; Greneche, J. M.; Ferey, G. *Inorg. Chem.* **1997**, *36*, 2187 and references therein.
(16) Loiseau, T.; Taulelle, F.; Ferey, G. *Micropor. Mater.* **1997**, *9*, 83 and references therein.
(17) Liu, Y.-H.; Lii, K.-H. Unpublished research.
(18) Moore, P. B. *Am. Mineral.* **1972**, *57*, 397.
(19) Meier, W. M.; Olson, D. H. *Atlas of Zeolite Structure Types*; Butterworth-Heinemann, Stoneham, MA, 1992.
(20) Huang, Y.-F.; Lii, K.-H. Unpublished research.
(21) Loiseau, T.; Ferey, G. *Eur. J. Solid State Inorg. Chem.* **1994**, *31*, 575.
(22) Huang, C.-Y.; Wang, S.-L.; Lii, K.-H. *J. Porous Mater.* **1998**, *5*, 147.
(23) Cavellec, M.; Riou, D.; Ferey, G. *J. Solid State Chem.* **1994**, *112*, 441.
(24) Millet, J. M. M.; Vedrine, J. C.; Hecquet, G. *Stud. Surf. Sci. Catal.* **1990**, *55*, 833.
(25) Estermann, M.; McCusker, L. B.; Baerlocher, C.; Merrouche, A.; Kessler, H. *Nature* **1991**, *352*, 320.
(26) Caullet, P.; Guth, J. L.; Hazm, J.; Lamblin, J. M.; Gies, H. *Eur. J. Solid State Inorg. Chem.* **1991**, *28*, 345.
(27) Loiseau, T.; Riou, D.; Taulelle, F.; Ferey, G. *Stud. Surf. Sci. Catal.* **1994**, *84*, 395.
(28) Wong, H.; Dieck, H. T.; O'Connor, C. J.; Sinn, E. *J. Chem. Soc., Dalton Trans.* **1980**, 786.
(29) DeBord, J. R. D.; Reiff, W. M.; Warren, C. J.; Haushalter, R. C.; Zubieta, J. *Chem. Mater.* **1997**, *9*, 1994.
(30) Zima, V.; Lii, K.-H.; Nguyen, N.; Ducouret, A. *Chem. Mater.* **1998**, *10*, 1914.
(31) Zima, V.; Lii, K.-H. *J. Solid State Chem.* In press.
(32) Lii, K.-H.; Huang, Y.-F. *J. Chem. Soc., Dalton Trans.* **1997**, 222.
(33) Chippindale, A. M.; Brech, S. J.; Cowley, A. R.; Simpson, W. M. *Chem. Mater.* **1996**, *8*, 2259.
(34) Cavellec, M.; Riou, D.; Ferey, G. *Acta Crystallogr.* **1995**, *C51*, 2242.
(35) DeBord, J. R. D.; Reiff, W. M.; Haushalter, R. C.; Zubieta, J. *J. Solid State Chem.* **1996**, *125*, 185.
(36) Jones, R. H.; Thomas, J. M.; Qisheng, H.; Xu, R.; Hursthouse, M. B.; Chen, J. *J. Chem. Soc. Chem. Commun.* **1991**, 150.
(37) Modaressi, A.; Courtois, A.; Gerardin, R.; Malaman, B.; Gleitzer, C. *J. Solid State Chem.* **1983**, *47*, 245.
(38) Parise, J. B. *Inorg. Chem.* **1985**, *24*, 4312.
(39) Lin, H.-M.; Lii, K.-H. *Inorg. Chem.* In press.
(40) Lii, K.-H.; Wang, S.-L. *J. Solid State Chem.* **1997**, *128*, 21.
(41) Hawthorne, F. *Acta Crystallogr.* **1994**, *B50*, 481.
(42) Moore, P. B.; Araki, T. *Am. Mineral.* **1977**, *62*, 692.
(43) Zima, V.; Lii, K.-H. Unpublished research.
(44) Hawthorne, F. *Z. Kristallogr.* **1990**, *192*, 1.
(45) Morgan, K.; Gainsford, G.; Milestone, N. *J. Chem. Soc. Chem. Commun.* **1995**, 425.
(46) Stalder, S. M.; Wilkinson, A. P. *Chem. Mater.* **1997**, *9*, 2168.
(47) Thomas, J. M.; Greaves, G. N.; Sankar, G.; Wright, P. A.; Chen, J.; Dent, A. J.; Marchese, L. *Angew. Chem., Int. Ed. Engl.* **1994**, *33*, 1871.
(48) Barrett, P. A.; Jones, R. H.; Thomas, J. M.; Sankar, G.; Shannon, I. J.; Catlow, C. R. A. *J. Chem. Soc. Chem. Commun.* **1996**, 2001.
(49) Chippindale, A. M.; Cowley, A. R. *Zeolites* **1997**, *18*, 176 and references therein.
(50) Feng, P.; Bu, X.; Stucky, G. D. *Nature* **1997**, *388*, 735 and references therein.
(51) Chippindale, A. M.; Bond, A. D.; Cowley, A. R.; Powell, A. V. *Chem. Mater.* **1997**, *9*, 2830.

CM980152H